Supplementary Materials

Microfluidic electrical impedance assessment of red blood cell mediated microvascular occlusion

Yuncheng Man [a, 1], Debnath Maji [b, 1], Ran An [a], Sanjay P. Ahuja [c], Jane A. Little [d], Michael A. Suster [b], Pedram Mohseni [b, e], Umut A. Gurkan [a, e, f]*

[a] Mechanical and Aerospace Engineering Department, Case Western Reserve University, Cleveland, OH 44106, USA

[b] Electrical, Computer, and Systems Engineering Department, Case Western Reserve University, Cleveland, OH 44106, USA

[c] Division of Hematology and Oncology, Rainbow Babies and Children's Hospital, Case Western Reserve University, Cleveland, OH 44106, USA

[d] Division of Hematology and Oncology, UNC Blood Research Center, Department of Medicine, University of North Carolina at Chapel Hill, Chapel Hill, NC 27599, USA

[e] Department of Biomedical Engineering, Case Western Reserve University, Cleveland, OH 44106, USA

[f] Case Comprehensive Cancer Center, Case Western Reserve University, Cleveland, OH 44106, USA

* Corresponding author:
Umut A. Gurkan, Ph.D.
Warren E. Rupp Associate Professor
Case Western Reserve University
10900 Euclid Ave., Cleveland, OH 44106
Phone: +1 (216) 368-6447
Email: umut@case.edu
Web: https://engineering.case.edu/profiles/uxg23

[1] These authors contributed equally.

Flow of fabrication process of the substrate ⟶

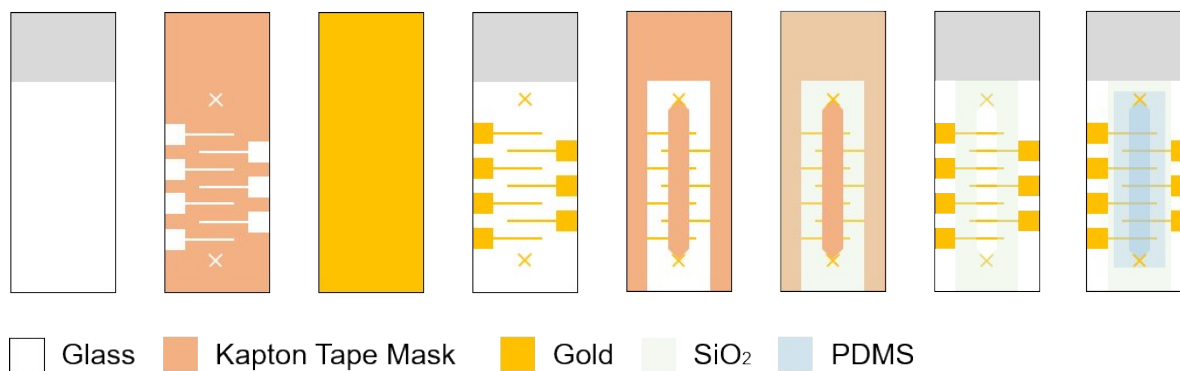Glass   Kapton Tape Mask   Gold   SiO₂   PDMS

Fig. S1. Schematic illustration of the device fabrication process. The gold electrodes were initially patterned under a Kapton tape mask on a standard microscope glass side, after which the SiO_2 was deposited under a secondary Kapton tape mask. Finally, PDMS was covalently bonded to the substrate. The cross marks were designed for micropillar array and gold electrode alignment. The titanium adhesion layer between the glass and gold is not shown.
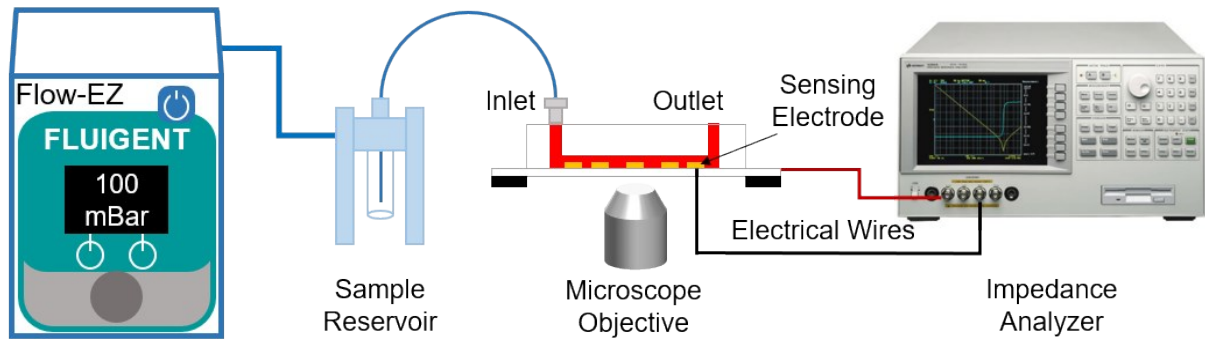
Fig. S2. Experimental setup. The RBC sample at 20% hematocrit is loaded in the sample reservoir and perfused through the microchannel for 20 min at 100 mBar using a Fluigent Flow-EZ pump with positive pressure. An impedance analyzer is connected to the device contact pads using electrical wires for impedance recording. The microfluidic device is mounted on the stage of an inverted microscope for image recording.
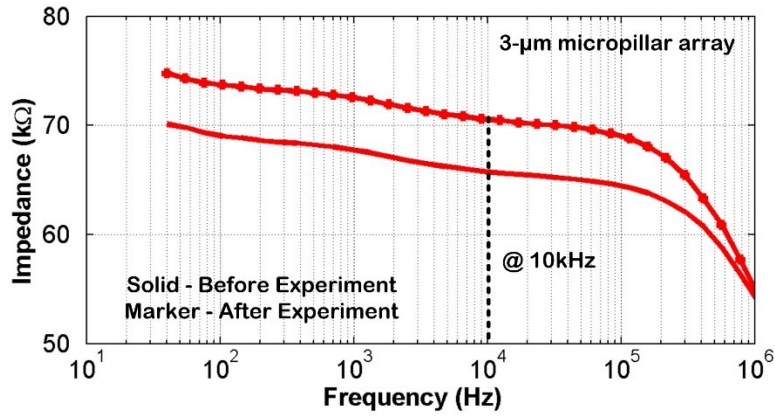
Fig. S3. Shown is the raw impedance data across the 3-µm micropillar array measured for a clinical blood sample. Magnitude of impedance across the micropillar array was recorded over the frequency range of 40 Hz–1 MHz before introducing blood into the microchannel (Solid Line) and after completing the washing step (Square Markers). Percentage change of impedance was analyzed at 10 kHz.
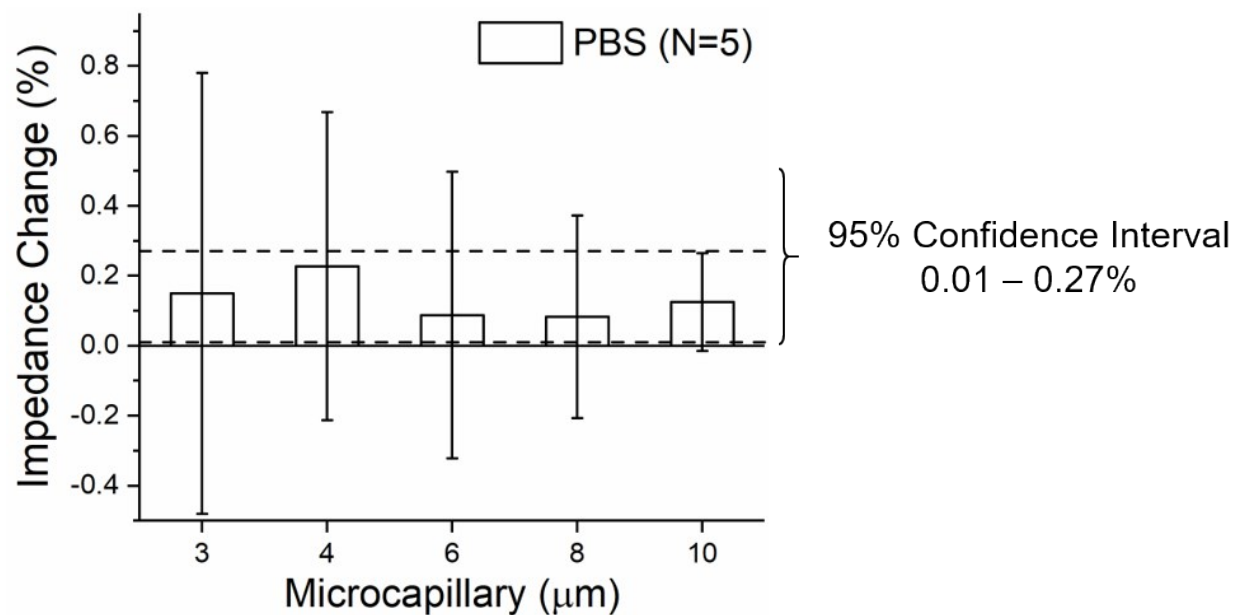
Fig. S4. Profiles of impedance change in the 3-μm to 10-μm micropillar arrays for testing PBS using 5 devices from different manufacturing batches. The 95% confidence interval of the impedance change data was determined as 0.01–0.27%, from which the background noise was determined. Error bars represent the standard deviation.
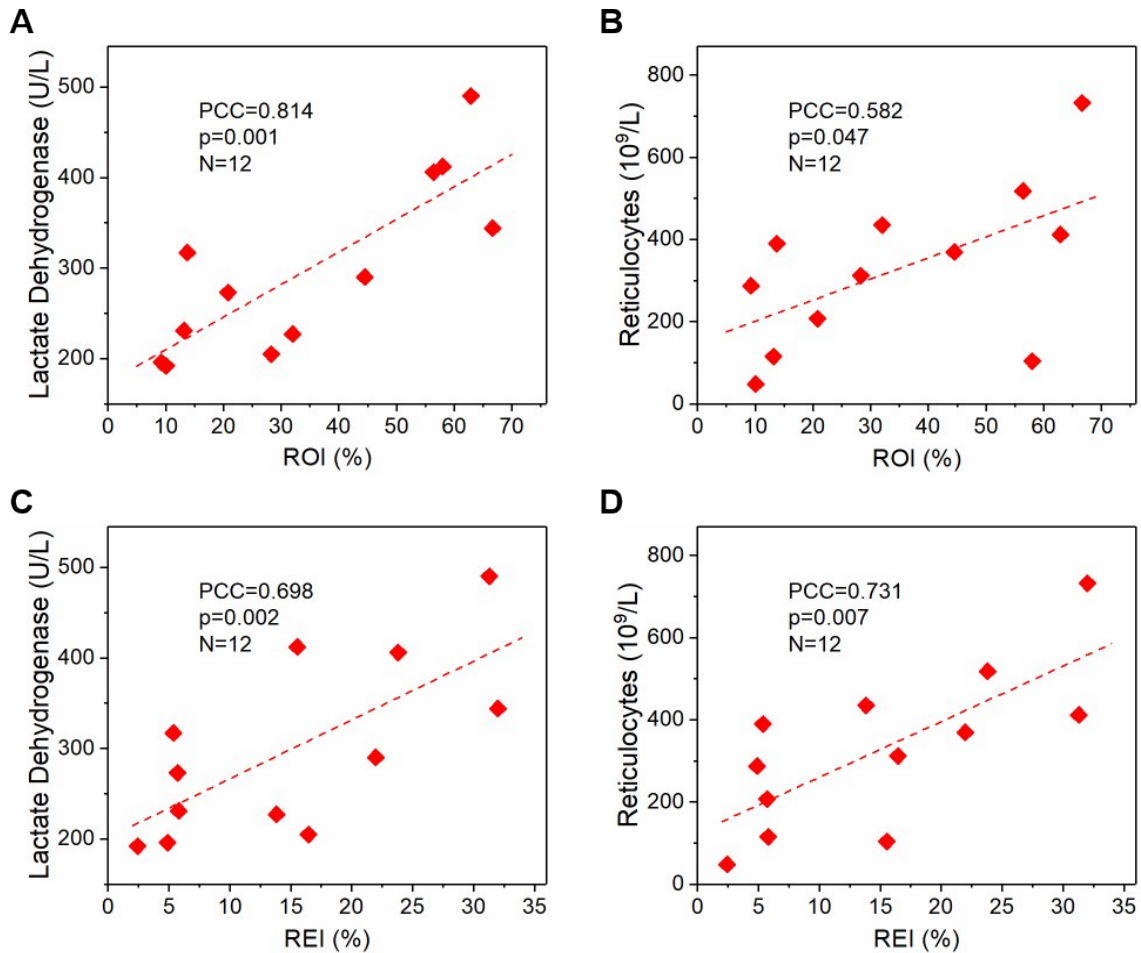
Fig. S5. The ROI and REI significantly correlate with *in vivo* hemolytic biomarkers in the study subjects with SCD. (A) The ROI significantly correlates with (A) serum lactate dehydrogenase (LDH) levels (PCC=0.814, p=0.001, N=12) and (B) absolute reticulocyte counts (ARCs) (PCC=0.582, p=0.047, N=12). Similarly, the REI significantly correlates with (C) serum LDH levels (PCC=0.698, p=0.002, N=12) and (D) ARCs (PCC=0.731, p=0.007, N=12). ROI: RBC Occlusion Index. REI: RBC Electrical Impedance Index. PCC: Pearson correlation coefficient.
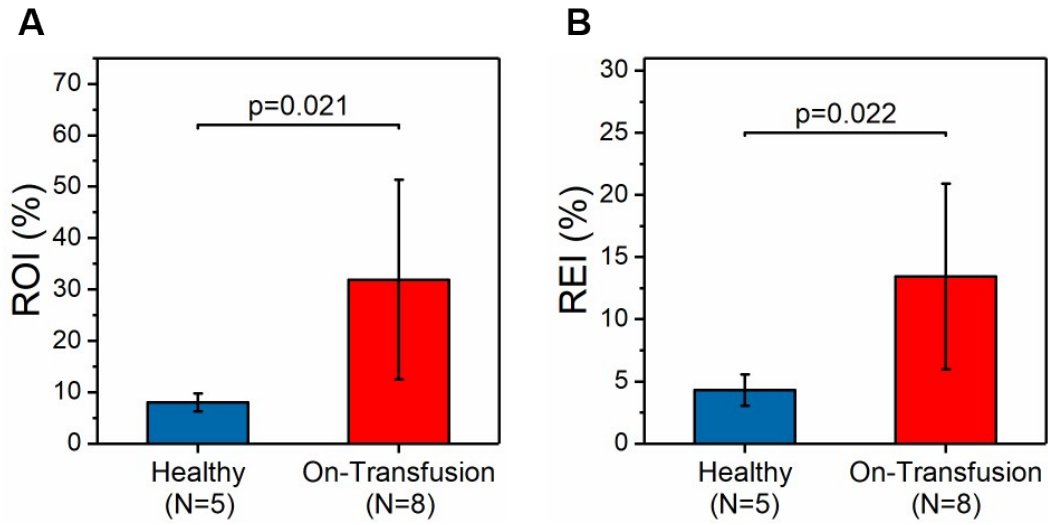
Fig. S6. Subjects with SCD on-transfusion (N=8) had significantly higher (A) ROI (p=0.021, one-way ANOVA) and (B) REI (p=0.022, one-way ANOVA) compared to healthy donors (N=5). ROI: RBC Occlusion Index. REI: RBC Electrical Impedance Index. Error bars represent standard deviation.
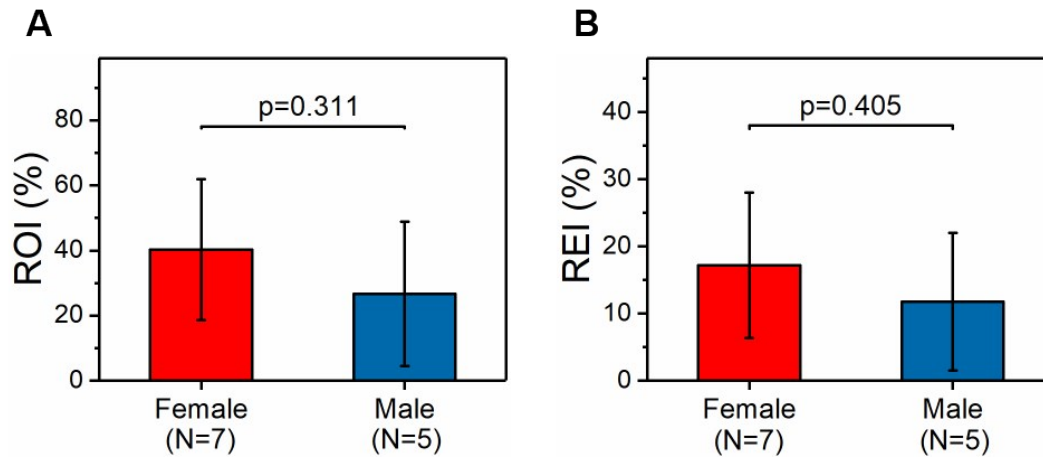
Fig. S7. No significance was observed in (A) ROI or (B) REI between females (N=7) and males (N=5) over the study population with SCD. ROI: RBC Occlusion Index. REI: RBC Electrical Impedance Index. Error bars represent standard deviation.

Table S1. Clinical variables of the study population with SCD.

Clinical variables	Range	Mean ± SD
ROI (%)	9.26 – 66.63	34.65 ± 21.99
REI (%)	2.44 – 32.01	14.93 ± 10.48
Age (years)	20 – 55	37 ± 10
Hemoglobin (g/dL)	6.2 – 12.1	8.56 ± 1.69
Hematocrit (%)	18.0 – 37.1	25.6 ± 5.1
White Blood Cell Count (10^9/L)	6.9 – 18.2	12.5 ± 3.5
Platelet Count (10^9/L)	130 – 528	346 ± 143
Absolute Neutrophil Count (10^6/L)	2360 – 12030	7526 ± 2738
Absolute Reticulocyte Count (10^9/L)	48 – 732	327 ± 194
Lactate Dehydrogenase (U/L)	192 – 490	299 ± 97
Ferritin (μg/L)	32 – 7640	3119 ± 2379
Hemoglobin S (%)	6.2 – 86.5	44.3 ± 24.7
Hemoglobin A (%)	5.2 – 74.9	42.5 ± 22.1
Hemoglobin F (%)	0.3 – 10.1	2.8 ± 3.0
Subjects on Transfusion	67% (8 out of 12)	

A total of 12 blood samples were obtained from 12 subjects with homozygous SCD (HbSS, total N=12, Male=5, Female=7).

ROI: RBC Occlusion Index.

REI: RBC Electrical Impedance Index.

SD: Standard deviation.

Table S2. Comparison of clinical variables between Group 1 and Group 2 subjects in SCD.

| Clinical variables	Group 1 (N=5) Mean ± SD	Group 2 (N=7) Mean ± SD	P-value
ROI (%)	**13.42 ± 4.57**	**49.81 ± 15.13**	**<0.001***
REI (%)	**4.84 ± 1.39**	**22.13 ± 7.40**	**0.006****
Age (years)	39 ± 9	35 ± 12	0.519*
Hemoglobin (g/dL)	9.3 ± 2.2	8.0 ± 1.1	0.200*
Hematocrit (%)	27.8 ± 6.4	23.9 ± 3.6	0.203*
White Blood Cell Count (10^9/L)	12.1 ± 2.5	12.7 ± 2.2	0.754*
Platelet Count (10^9/L)	270 ± 145	400 ± 123	0.125*
Absolute Neutrophil Count (10^6/L)	7666 ± 1760	7426 ± 3413	0.889*
Absolute Reticulocyte Count (10^9/L)	**209 ± 136**	**412 ± 192**	**0.037****
Lactate Dehydrogenase (U/L)	**242 ± 53**	**339 ± 105**	**0.052****
Ferritin (µg/L)	4109 ± 3050	2413 ± 1666	0.240*
Hemoglobin S (%)	44.4 ± 27.4	44.2 ± 24.9	0.992*
Hemoglobin A (%)	42.8 ± 25.8	42.3 ± 21.3	0.971*
Hemoglobin F (%)	2.6 ± 4.2	2.9 ± 2.2	0.223**

ROI: RBC Occlusion Index.

REI: RBC Electrical Impedance Index.

SD: Standard deviation.

*: one-way ANOVA

**: Mann-Whitney
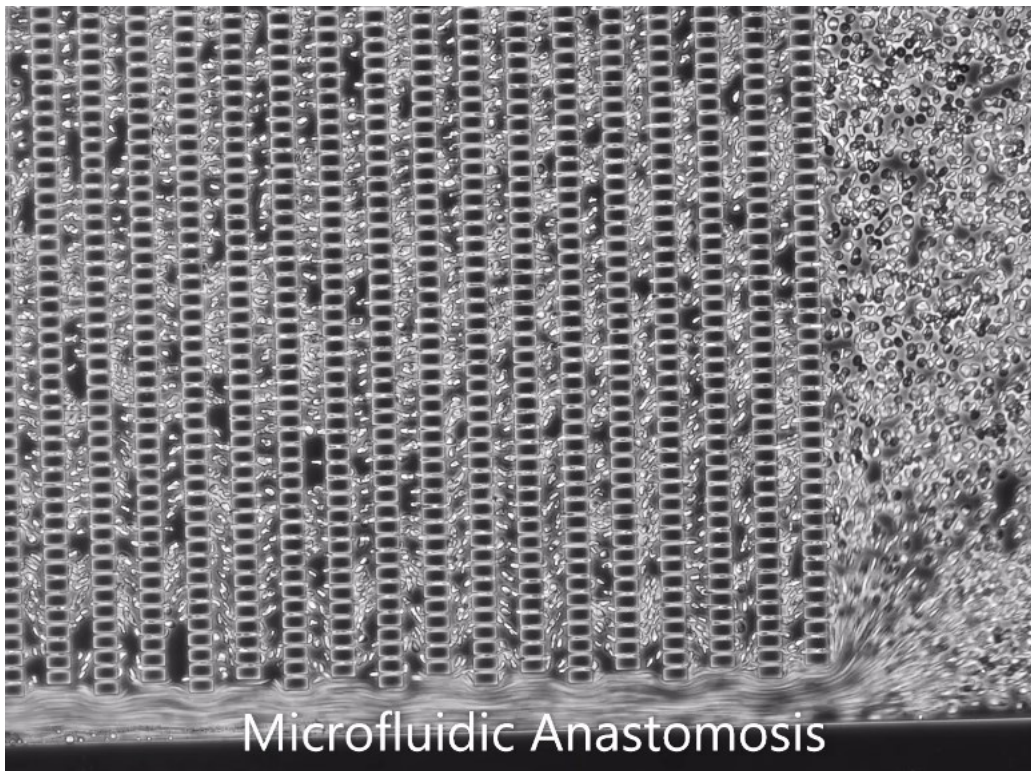
Video S1. The video demonstrates the role of the micropillar array (with 3-µm microcapillaries) as a mechanical retention mechanism, and the microfluidic anastomosis for preventing microchannel clogging.